All-optical delay of images by backward four-wave mixing in metal-nanoparticle composites

K.-H. Kim, A. Husakou,* and J. Herrmann

Max Born Institute of Nonlinear Optics and Short Pulse Spectroscopy, Max Born Str 2a, D-12489 Berlin, Germany

(Received 27 March 2013; revised manuscript received 17 April 2013; published 26 April 2013)

We theoretically study a method for all-optical delay of images based on backward four-wave mixing in composites containing metal nanoparticles. In this approach a delayed phase-conjugate probe pulse is generated by the interaction of two counterpropagating pump beams and a noncollinear shaped probe pulse in the nanocomposite. The fractional delay and the reflectivity for the phase-conjugate signal pulses are studied as functions of the input pump intensity. It is shown that this scheme can be used for delayed imaging combined with the elimination of optical diffraction. The advantages of this method include miniaturized design, tunable wavelength range up to the telecommunication range, and wide bandwidth.

DOI: 10.1103/PhysRevA.87.045805 PACS number(s): 42.30.Va, 42.65.Hw, 42.70.Mp

Recent progress in the development of slow-light devices has paved the way towards promising applications in storing, switching, and processing optical signals and increased resolution of spectroscopic interferometers, as well as applications in many other fields, e.g., nonlinear optics and quantum optics (see, e.g., [1]). Recently it has been demonstrated that instead of single light pulses, two- or three-dimensional images may also be slowed and stored. All-optical methods for delaying images can find applications in holography and optical pattern correlation measurements or all-optical image routers. The ability to slow images and delay them was demonstrated by using the effect of electromagnetically induced transparency (EIT) [2–6] and coupled image resonators [7,8]. Further methods include delayed images achieved in liquid crystal media [9] and dye-doped chiral liquid crystals [10]. Applications in this field require methods for all-optical delay of images at arbitrary wavelengths (in particular at telecommunication wavelengths), large delay-bandwidth products, short (picosecond) pulse durations, and a design suitable for on-chip integration. Recently we proposed an approach for a slow light device based on the coherent interaction between pump and probe pulses in composite materials doped with metal nanoparticles [11]. In such materials near the plasmon resonance the absorption becomes saturated due to the shift of the plasmonic resonance [12,13]. Therefore in a pump-probe regime an absorption dip in the homogenous plasmonic absorption profile and a steep change of the effective refraction index near the probe wavelength are created, leading to a significantly lower group velocity of the probe. In a noncollinear configuration with a TiO_2 film doped with silver nanorods a large optical delay with a delay-bandwidth product of more than 60 for picosecond pulses at 1550 nm has been predicted.

Besides diverse other methods, backward degenerate four-wave mixing (DFWM) has also been studied for the realization of slow light in photorefractive crystals [14–17]. The main drawback of slow light by using photorefractive materials is the very large response time, leading to a severely limited bandwidth. Backward DFWM results in phase conjugation [18] which is an important technique for imaging applications. In this Brief Report, we study an approach for all-optical delay applicable also to the delay of images based on composite materials doped with metal nanoparticles (NPs) and backward DFWM. In this scheme two counterpropagating pump pulses and an initial noncollinear pulse-shaped probe pulse excite the nanoparticle composite (see Fig. 1). As the result of the nonlinear interaction, a signal wave which is phase conjugate with respect to the probe wave is generated. Due to the retarded nonlinear response of the metal nanoparticles in the picosecond-scale time range an absorption dip and a corresponding steep change of the refraction index lead to a delay of the signal wave. This process can be used for delayed imaging. We note that an alternative two-wave mixing design is possible, whereby the probe beam is strong enough to induce the nonlinear grating without the pump beams but is likely to produce stronger image distortion due to the time-dependent strength of the induced grating and delay.

First, we study the mechanism of slow light in metal nanocomposites by using backward degenerate four-wave mixing. As presented schematically in Fig. 1 we consider a slab with a metal-NP composite illuminated by two counterpropagating quasi-cw pump beams $\mathbf{E}_1$ and $\mathbf{E}_2$ and a noncollinear probe pulse $\mathbf{E}_{\mathrm{pr}}$, which has an arbitrary spatial amplitude and phase distribution. The three beams have the same central frequency and are assumed to be s-polarized. Then an s-polarized signal pulse $\mathbf{E}_s$ is generated through the DFWM process. Since the two pump beams propagate along the opposite directions ($\mathbf{k}_1 = -\mathbf{k}_2$), and the signal wave is phase conjugate with respect to the probe ($\mathbf{k}_3 = -\mathbf{k}_4$), the phase-matching condition is automatically satisfied. A main feature in the optical response of the metal composite in the spectral range of plasmon resonance is the enhancement of the local electric field in the vicinity of the NPs. In this work we consider the excitation by picosecond pulses, therefore the transient response of the metal NPs is mainly influenced by electron-phonon processes and determined by the electron thermalization and the cooling of the hot electrons through the thermal exchange with the lattices in the metal. We consider pump fluences below 0.1 J/cm^2 which typically do not lead to damage and melting during excitation by ps pulses. Using the two-temperature model, the nonlinear change of the dielectric function of the metal can be described as [19]

$$\Delta\varepsilon_m(t) = \frac{\chi_m^{(3)}}{\tau_{ep}} \int_{-\infty}^{t} |E(t')|^2 e^{-\frac{t-t'}{\tau_{ep}}} dt', \qquad (1)$$

*gusakov@mbi-berlin.de

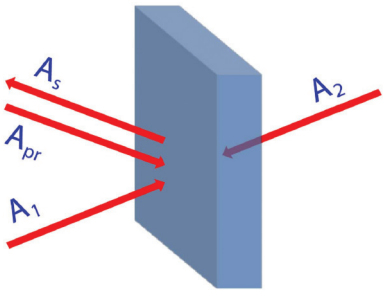

FIG. 1. (Color online) Optical configuration for DFWM-based optical delay.

where τ_{ep} is the electron-phonon coupling time in the range of 1–3 ps [20], $\chi_m^{(3)}$ is the inherent third-order nonlinear susceptibility of the metal NPs at the pump wavelength ω_0 and $E(t)$ is local total field at the nanoparticles enhanced by the plasmon resonance. We note that Eq. (1) is written for the time-dependent field $E(t)$, and that the frequency dependence of $\chi_m^{(3)}$ is weak. The choice of the system is determined by a relatively large value of the τ_{ep} which leads to a sharp feature in the transmission and correspondingly low group velocity.

With the slowly varying amplitudes of each beam $\mathbf{A}_1$, $\mathbf{A}_2$, $\mathbf{A}_{pr}$, and $\mathbf{A}_s$ the total electric field is given by $\mathbf{E}(\mathbf{r},t) = \mathbf{A}_1 e^{i\mathbf{k}_1\mathbf{r}-i\omega t} + \mathbf{A}_2 e^{i\mathbf{k}_2\mathbf{r}-i\omega t} + \mathbf{A}_{pr}(z,t)\, e^{i\mathbf{k}_3\mathbf{r}-i\omega t} + \mathbf{A}_s(z,t)\, e^{i\mathbf{k}_4\mathbf{r}-i\omega t} + \text{c.c.}$ We assume that the intensity of both quasi-cw pump beams is much higher than those of the probe and signal waves, and their depletion is neglected. Neglecting dispersion and using the slowly varying envelope approximation and Eq. (1), the propagation of signal and probe pulses can be described in the frequency domain as follows:

$$\begin{aligned} \partial A_s(\Omega,z)/\partial z &= -\frac{\Delta_\perp}{2k_0} A_s + a(z) A_s + b(z) A_{pr}^*, \\ \partial A_{pr}(\Omega,z)/\partial z &= -\frac{\Delta_\perp}{2k_0} A_{pr} + b(z) A_s^* - a(z) A_{pr}, \end{aligned} \tag{2}$$

where $A_s(\Omega,z,x,y)$ and $A_{pr}(\Omega,z,x,y)$ are amplitudes of signal and probe pulses, z is the coordinate along $\mathbf{k_4}$, x,y are the coordinates normal to the direction of $\mathbf{k_4}$, $\Delta_\perp = \partial^2/\partial x^2 + \partial^2/\partial y^2$, $k_0 = 2\pi/\omega_4$, $b = 2i\delta(z)A_1A_2/(1 - i\Omega\tau_{ep})$, and

$$a = i\delta(z)(|A_1|^2 + |A_2|^2)\left(1 + \frac{1}{1 + i\Omega\tau_{ep}}\right) - \alpha/2, \tag{3}$$

Here A_1 and A_2 are the input amplitudes of the two pump waves, $\delta(z) = \omega_0 \chi_{\text{eff}}^{(3)}/2c\, \text{Re}\sqrt{\varepsilon_{\text{eff}}(\omega_0)}\cos\theta$ inside the sample and $\delta(z) = 0$ outside the sample, $\alpha = 2\,\text{Im}\sqrt{\varepsilon_{\text{eff}}(\omega_0)}\omega_0/c$ is the linear absorption coefficient, θ is the half intersecting angle between vectors $\mathbf{k_1}$ and $\mathbf{k_3}$, and $\varepsilon_{\text{eff}}(\omega_0)$ is the linear effective dielectric function of the composite. For spherical particles with diameters smaller than 10 nm the nonlinear field enhancement factor x in the frequency domain is given by the implicit relation (see Ref. [11])

$$x = \frac{3\epsilon_h}{\varepsilon_{m0} + 2\varepsilon_h + \chi_m^{(3)}|xE(\omega_0)|^2}, \tag{4}$$

which is solved numerically, and the effective third-order susceptibility of the metal nanocomposite is calculated by $\chi_{\text{eff}}^{(3)} = f\chi_m^{(3)}|x|^2 x^2$, where $\chi_m^{(3)}$ is that of the metal and f is the volume filling factor of the NPs. Here ε_{m0} and ε_h are the permittivities of the metal and the host, respectively, and $\varepsilon_{\text{eff}}(\omega_0)$ is determined by the generalized Maxwell-Garnett formula including the intensity dependence of x given by Eq. (4). For spherical NPs with large diameter and nonspherical NPs we calculate the enhancement factor x and $\varepsilon_{\text{eff}}(\omega_0)$ by using the generalized discrete dipole approximation modified to include nonlinear saturation effects (see Ref. [13]).

In order to characterize the pulse shape change we use the distortion function D of the probe pulse defined by [21]

$$D = \sqrt{\frac{\int_{-\infty}^{\infty} |I_{\text{out}}(t+\Delta t) - I_{\text{in}}(t)|\, dt}{\int_{-\infty}^{\infty} I_{\text{out}}(t+\Delta t)\, dt}}, \tag{5}$$

where I_{in} and I_{out} are normalized input and output probe pulse intensities, respectively, and Δt is the peak delay time.

By using the above described formalism we now demonstrate the slow light mechanism by using backward DFWM and metal nanocomposites. For a simplified numerical approach using the Maxwell-Garnett model we consider first a TiO_2 composite containing spherical silver NPs with diameters of 10 nm which exhibit a plasmon resonance at around 610 nm. In Fig. 2 the fractional delay (a), the phase-conjugate reflectivity (b), and the pulse distortion (c) are shown as functions of the medium length normalized by the effective length $L_{\text{eff}} = 1/\alpha$ and the pump intensity at 625 nm. The probe pulse duration is 1 ps. For our slowing mechanism to work, this time cannot be much smaller than the nonlinearity response time. We assume the same intensity of the both counterpropagating, normally incident ($\theta = 0$) pump beams and an electron-phonon response time of $\tau_{ep} = 1$ ps. In this case, the effective length is $L_{\text{eff}} = 90.2\ \mu$m. Figure 2 shows that by using this configuration the maximum fractional delay (defined as delay divided by input probe duration) can be in the range of 1 with reflectivity up to more than 0.5 for a pump intensity lower than 8 MW/cm^2. The distortion D is about 0.6.

Let us now study the possibility to use backward DFWM in metal nanocomposites for the purpose of image delay. To demonstrate this mechanism at telecommunication wavelengths, which are important for applications, we have chosen a 4.1-μm-thick TiO_2 film containing randomly oriented gold nanorods with a diameter of 22 nm and a length of 64 nm with a filling factor of 10^{-3}. The elongated shape of the nanorods leads to the shift of the resonant value of the linear dielectric function from a resonant value of -2 characteristic of the spherical nanoparticles. For these nonspherical NPs we use for the numerical simulations the discrete dipole approximation modified to include nonlinear saturation effects [13]. The effective nonlinear susceptibility for gold at the wavelength of 1550 nm is $\chi_3 = -1.5 \times 10^{-11}$ m^{2}V^{-2} [22]. Due to field enhancement and the extremely large inherent nonlinearity of gold at 1550 nm, a pump intensity of normally incident pulses of only 30 kW/cm^2 is sufficient. Figure 3 shows for an object with a total area of 0.32×0.32 mm^2 shown in Fig. 3(a), which determines the initial conditions of Eqs. (2), the delayed image obtained by the backward DFWM [Fig. 3(c)]

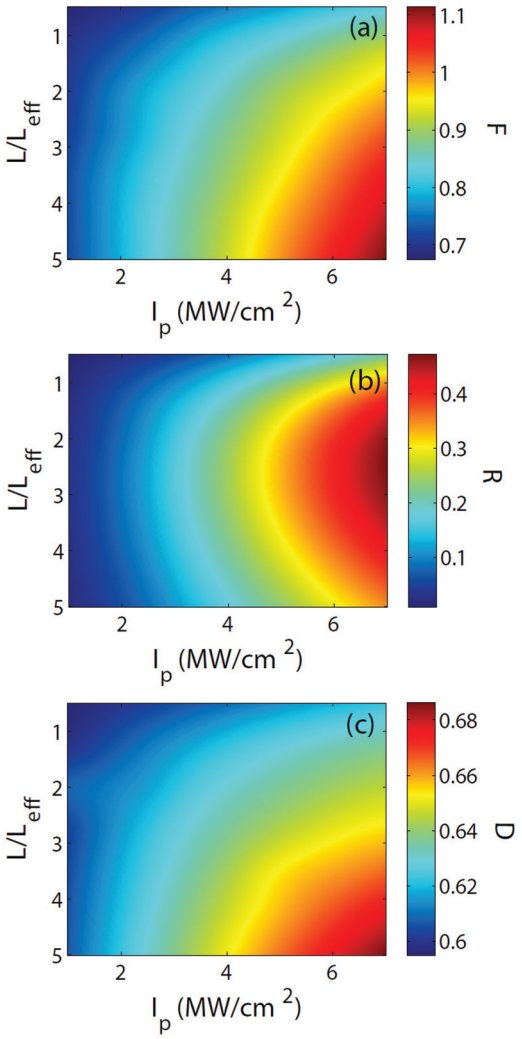

FIG. 2. (Color online) Slow light by DFWM in TiO_2 layer containing Ag NPs smaller than 10 nm with filling factor of 10^{-4}: (a) fractional delay F, (b) conjugate reflectivity R, and (c) pulse distortion.

as well as the distorted image after propagation over the same distance of 0.5 mm in free space without phase conjugation by the composite [Fig. 3(b)].

One of the main advantages of this process is that it provides optical phase conjugation [18,23]. A peculiar property of the phase conjugation in the metal-dielectric composite is that it permits both image reconstruction *and* optical delay, a combination not commonly found in other schemes for image delay. As can be seen from the figure without phase conjugation, diffraction effects are noticeable already after

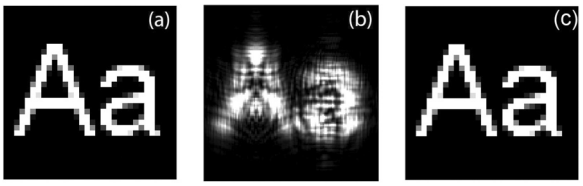

FIG. 3. Delayed image (c) by optical phase conjugation with DFWM and diffracted image (b) in free space with the same propagation length at telecommunication wavelength 1550 nm for the object shown in (a). The nonlinear material is a TiO_2 layer doped with randomly oriented Ag nanorods with a diameter of 22 nm and a length of 64 nm. The image is positioned 0.5 mm from the sample.

0.5 mm of propagation resulting in the significant distortion of the image, since the characteristic size of the source features is only 10 microns. However, as shown in Fig. 3(c), phase conjugation by the composite medium reverses the curvature of the wavefront, resulting in a reconstruction of the object after propagation over 0.25 mm. We note that our simplified model does not describe the distortions and imperfections of the phase-conjugation process, therefore the reproduced image is identical to the source. The resultant fractional delay of the image in Fig. 3(c) is about 0.75.

The minimum size of the spatial features which can be transferred from source to image is determined by several limitations of the considered system. In particular, in our model all beam components with different normal wave vectors are characterized by the same transmission calculated at the central value. For broad beams, this is no longer true, leading to limitation of the maximum transmittable feature of roughly 3 μm. Transmission of features below this value can be achieved for larger values of medium thickness L or for correspondingly reduced filling fraction f, at the cost of reduced delay of the image.

To conclude, we have investigated all-optical delay by backward DFWM in metal nanocomposite materials. A fractional delay of a signal pulse has been predicted in the range of unity in both visible and telecommunication wavelength ranges. In particular, at telecommunication wavelength a weak pump intensity on the order of 30 kW/cm^2 can be applied for slowing down the optical pulses. Due to the optical phase-conjugation property of the signal beam with regard to the probe, all-optical delay of images can be realized. The advantage of the proposed technique comprises miniaturized design, wide bandwidth reaching up to THz, and control of the central wavelength by changing the sizes and shapes of the metal nanoparticles. The optical delay can be further increased by a thicker nanocomposite with lateral pump incidence as proposed in [11] or by several parallel composite slabs.

[1] J. B. Khurgin and R. S. Tucker (eds.), *Slow Light: Science and Applications* (CRC Press, Boca Raton, 2008).

[2] R. M. Camacho, C. J. Broadbent, I. Ali-Khan, and J. C. Howell, Phys. Rev. Lett. **98**, 043902 (2007).

[3] R. Pugatch, M. Shuker, O. Firstenberg, A. Ron, and N. Davidson, Phys. Rev. Lett. **98**, 203601 (2007).

[4] M. Shuker, O. Firstenberg, R. Pugatch, A. Ron, and N. Davidson, Phys. Rev. Lett. **100**, 223601 (2008).

[5] O. Firstenberg, M. Shuker, N. Davidson, and A. Ron, Phys. Rev. Lett. **102**, 043601 (2009).
[6] P. K. Vudyasetu, R. M. Camacho, and J. C. Howell, Phys. Rev. Lett. **100**, 123903 (2008).
[7] M. Tomita, P. Sultana, A. Takami, and T. Matsumoto, Opt. Express **18**, 12599 (2010).
[8] P. Sultana, A. Takami, T. Matsumoto, and M. Tomita, Opt. Lett. **35**, 3414 (2010).
[9] S. Residori, U. Bortolozzo, and J. P. Huignard, Phys. Rev. Lett. **100**, 203603 (2008).
[10] D. Wei, S. Residori, and U. Bortolozzo, Opt. Lett. **37**, 4684 (2012).
[11] K.-H. Kim, A. Husakou, and J. Herrmann, Opt. Express **20**, 25790 (2012).
[12] R. A. Ganeev, Opt. Quantum Electr. **36**, 949 (2004).
[13] K.-H. Kim, A. Husakou, and J. Herrmann, Opt. Express **18**, 21918 (2010).
[14] B. Sturman, P. Mathey, R. Rebhi, and H.-R. Jauslin, J. Opt. Soc. Amer. B **26**, 1949 (2009).
[15] P. Mathey, G. Gadret, and K. Shcherbin, Phys. Rev. A **84**, 063802 (2011).
[16] E. Podivilov, B. Sturman, A. Shumelyuk, and S. Odoulov, Phys. Rev. Lett. **91**, 083902 (2003).
[17] G. Zhang, F. Bo, R. Dong, and J. Xu, Phys. Rev. Lett. **93**, 133903 (2004).
[18] G. S. He, Prog. Quantum Electron. **26**, 131 (2002).
[19] K.-H. Kim, U. Griebner, and J. Herrmann, Opt. Lett. **37**, 1490 (2012).
[20] J.-Y. Bigot, V. Halté, J.-C. Merle, and A. Daunois, Chem. Phys. **251**, 181 (2000).
[21] H. Shin, A. Schweinsberg, G. Gehring, K. Schwertz, H. J. Chang, R. W. Boyd, Q.-H. Park, and D. J. Gauthier, Opt. Lett. **32**, 906 (2007).
[22] E. L. Falcão-Filho, R. Barbosa-Silva, R. G. Sobral-Filho, A. M. Brito-Silva, A. Galembeck, and Cid B. de Araújo, Opt. Express **18**, 21636 (2010).
[23] A. Yariv and D. M. Pepper, Opt. Lett. **1**, 16 (1977).